Paper:

Liang, J., Li, M., Zhu, J., Zong, H., Zhang, Y., Jain, S. & Wang, Z. (2019). Detrimental effect of silver doping in spiro-MeOTAD on the devie performance of perovskite solar cells. *Organic Electronics*

http://dx.doi.org/10.1016/j.orgel.2019.03.036

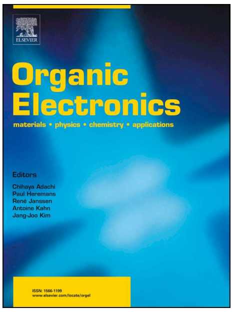

Detrimental effect of silver doping in spiro-MeOTAD on the devie performance of perovskite solar cells

Jing-Jing Liang, Meng Li, Jun-Yi Zhu, Hao Zong, Yue Zhang, Sagar M. Jain, Zhao-Kui Wang

PII: S1566-1199(19)30145-4
DOI: https://doi.org/10.1016/j.orgel.2019.03.036
Reference: ORGELE 5174

To appear in: *Organic Electronics*

Received Date: 16 February 2019
Revised Date: 16 March 2019
Accepted Date: 21 March 2019

Please cite this article as: J.-J. Liang, M. Li, J.-Y. Zhu, H. Zong, Y. Zhang, S.M. Jain, Z.-K. Wang, Detrimental effect of silver doping in spiro-MeOTAD on the devie performance of perovskite solar cells, *Organic Electronics* (2019), doi: https://doi.org/10.1016/j.orgel.2019.03.036.

Graphic Abstract

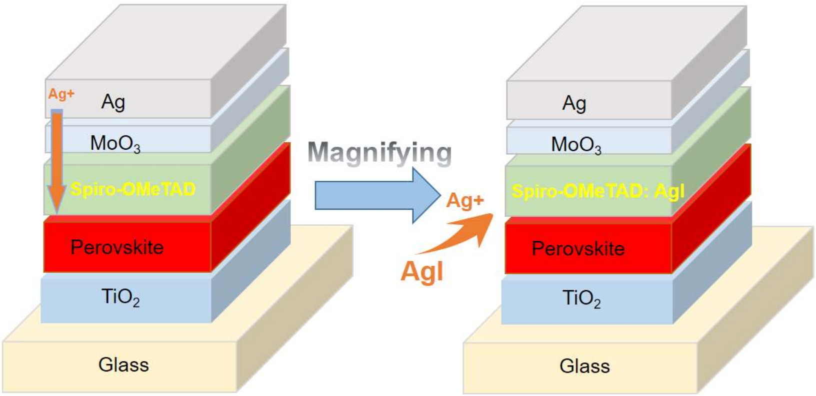

Detrimental effect of silver doping in spiro-MeOTAD on the devie performance of perovskite solar cells

Jing-Jing Liang[a], Meng Li[a], Jun-Yi Zhu[a], Hao Zong[a], Yue Zhang[a], Sagar M. Jain[b], and Zhao-Kui Wang[a*]*

[a]Institute of Functional Nano & Soft Materials (FUNSOM), Institute of Functional Nano & Soft Materials (FUNSOM), Collaborative Innovation Center of Suzhou Nano Science and Technology, Soochow University, Suzhou, Jiangsu 215123, China.

[b]Specific, College of Engineering, Swansea University Bay Campus, Fabian Way, SA1 8EN Swansea, United Kingdom.

Corresponding Authors:

s.m.jain@swansea.ac.uk (Sagar M. Jain). zkwang@suda.edu.cn (Z. K. Wang)

ABSTRACT: Despite hybrid organic-inorganic perovskite solar cells (PSCs) have reached a rapid improvement in solar cell efficiency. The long-term operational stability of PSCs is still under course of development. Here, we investigated the infiltration effects of Ag^+ into the adjacent hole transporting layer (HTL) in the PSCs, by directly doping Ag^+ into the conventional Spiro-MeOTAD layer (HTL) and the essential characterization analysis were also applied. The result distinctly demonstrated that the Ag-ion migration potentially triggers the performance degradation in PSCs. The incorporation of Ag^+ brought deep-level defects in the Spiro-MeOTAD layer and consequently caused a deterioration of the hole-transporting ability of Spiro-MeOTAD leading to degradation of solar cell performance. Understanding the impacts of the metal electrode penetration in the HTL will promote advancing in the overall stability performance of PSCs.

KEYWORDS: Perovskite solar cells; Hole-transporting layer; Spiro-OMeTAD; Stability.

1. Introduction

The cost of photovoltaics falls 80% in the last five years, especially for few developing countries where the cost is tumbles to the new low record making it cheaper than the cost of fossil-fuel consumed by coal-fired power plants. There is an unprecedented, rapid and exponential development in PCE of perovskite solar cells. The present power conversion efficiency of perovskite solar cells has exceeded 23% [1], which is close to the commercial polycrystalline silicon solar cells. This improvement of performance achieved in relative short time amazes scientific community and researchers working in the photovoltaic field. The multidimensional perovskite absorber is a crystalline material with ABX_3 formula, where A is a monovalent cation (either Methylammonium, MA; Formamidinium, FA or Cesium, Cs), B is a divalent metal, such as Sn or Pb and X is I, Br, or Cl. The perovskite materials have been well-known for a time because of their strong light absorption across almost all visible wavelengths, long exciton diffusion lengths, long charge carrier lifetimes and high carrier mobilities that contribute to exceptional power conversion efficiencies (PCE). In less than a decade timespan, PSCs have rapidly developed from the 3% PCE in 2009 [2] to over 23% presently [3]. However, with the continuous improvement of perovskite solar cell efficiency record, its long-term stability is still considered as one of the main challenges to address for the commercialization of the PSCs.

PSCs show that temperature, moisture, oxygen and illumination (light exposure) are notorious for maintaining performance over extended period [4-8]. Most often the degradation of perovskite active layer is considered as the main cause of degradation of overall device [9-13]. However, the issue of operational stability is still an inevitably challenge even when the optimum environment is provided to avoid the decomposition of the perovskite absorber layer [14-17]. This suggests that other than the degradation of perovskite-active layer, the interfacial degradation of the charge-transporting layers can also account for the stability of PSCs. Recently, there has been more attention payed to the conventional organic hole-selective layer commonly known as 2,2′,7,7′-tetrakis-(N,N-di-p-methoxyphenylamine)-9,9′-spirobifluorene (Spiro-OMeTAD) for the stability of PSCs. For instance, it is shown that the hygroscopic salt dopants (Lithium bis(trifluoromethanesulfonyl)imide (LiTFSI) and 4-tert-butyl pyridine (tBP)) affect negatively the stability of solar cells [18,19]. Furthermore, it was experimentally confirmed that MA^+ and I^- ions penetrate from the perovskite layer into the adjacent organic HTL and induce energy disorder that causes reduced conductivity in the Spiro-OMeTAD layer leading to the performance drop of PSCs [20]. Similarly, the metal ion electrode penetration into the organic HTL to an extend contributes to the degradation of PSCs. Domanski et al. [21] demonstrated that gold migration induced degradation of perovskite active layer that is caused through the hole-transporting layer (HTL) and into the perovskite material, which consequently does harm to the device performance metrics under working conditions. However, in terms of the high-cost Au, as another low-cost alternative, sliver has been used as the cathode for PSCs. Undeniably, there does exist some disadvantages that include relatively low PCE and bad stability for Ag electrode, compared with Au electrode. Especially, in operational stability this is clear from reported studies that pointed out Ag corrosion severely affects the performance of perovskite solar cells [22-24]. It is confirmed that porous Spiro-OMeTAD allows migration of MA^+ and I^- through it causing corrosion of Ag electrodes on the surface due to formation of silver iodide [25]. However, considering the ion motion mechanism, we cannot also ignore another possibility---the Ag electrode penetration, which is possibly potential affecting factor for the device long-term stability.

Herein, we fabricated perovskite solar cell devices with Ag electrodes and stored them under the dark condition in ambient air and dry N_2. In order to investigate the effects of Ag electrode penetration into the adjacent hole transporting layer (HTL) in the PSCs, we directly doped AgI into the Spiro-OMeTAD layer (HTL) to magnify the effects, by dissolving AgI in dipropyl sulfide and later adding it into Spiro-OMeTAD solutions. Also, the essential characterization and stability measurements were applied for comparing the difference between the undoped and doped devices.

2. Experimental Details

2.1 Material and Solution Preparation

Titanium tetrachloride, Lithium bis(trifluoromethanesulfonyl)imide (Li-TFSI) and 4-tert-butylpyridine (tBP) were purchased from Sigma-Aldrich. Lead iodide (PbI_2, 99.99%), Silver iodide (AgI, 99.99%) and chlorobenzene were obtained from Alfa Aesar Ltd. Spiro-OMeTAD was purchased from 1-Material Ltd. The precursor solution was prepared by dissolving MAI:PbI_2 (1.2 mol: 1.2 mol) in 1 mL coalescing solvents of dimethyl sulfoxide (DMSO) and 1,4-butyrolactone (GBL) (3:7, v/v) to make $MAPbI_3$ solution. Spiro-OMeTAD precursor was obtained by dissolving in chlorobenzene, which Li-TFSI and tBP were added into about two hours later. Then AgI, which was dissolved in Dipropyl sulfide, was added to Spiro-OMeTAD solutions for doping.

2.2 Device Fabrication

As a substrate, fluorine-doped tin oxide (FTO) coated glass (~ 15 Ω/sq) was sequentially cleaned in neutral detergent, acetone, and ethanol in ultrasonic cleaning machines for 15 min. After UV ozone treatment for 20 min, the substrate was covered with a compact 100 nm TiO_2 layer by using titanium tetrachloride ($TiCl_4$) and water as the precursors of solution deposition at 70 °C for 1 h. And then, the perovskite solution was added onto the TiO_2 layer by a consecutive two-step spin-coating process at 2000 and 4000 rpm for 20 and 40 s, respectively, where a chlorobenzene drop-casting was carried out as an anti-solvent 40 secs later. Afterwards, the film was annealed at 100 °C for 10 min in nitrogen glove box. The Ag^+-doped or undoped Spiro-OMeTAD solutions were then spin-coated onto the perovskite layer at 5000 rpm for 40 s. After air-oxidation for 15 h, the device was finally added with electrodes for MoO_3 (8 nm) and Ag (100 nm) by vacuum-evaporating at a rate of 0.2 and 3 $Å\ s^{-1}$, respectively. The active area of each device was 9 mm^2 defined through a shadow mask.

2.3 Device Characterization

Current density-voltage characteristics of perovskite solar cells under 1 sun illumination were performed using a programmable Keithley 2400 source meter under AM 1.5G solar irradiation at 100 mW/cm^2 with constant and low scan speed of 0.1 mV/S (Newport, Class AAA solar simulator, 94023A-U). The optical microscopy images (OM, Leica DM4 M) were achieved to display surface morphology. Also, atomic force microscopy images were obtained using a Veeco Multimode V instrument to evaluate the surface morphology of films in tapping mode. XRD patterns of the perovskite films were performed by PANalytical 80 equipment (Empyrean, Cu Ka radiation). The absorption spectra of perovskite films were obtained by a UV-vis spectrophotometer (PerkinElmer Lambda 750). The stability of the devices was evaluated after exposure to ambient air without any wrap (12% for Humidity and 20℃ for temperature). The consistency of each test condition is ensured in the test process.

3. Results and Discussion

The perovskite solar cells (PSCs) were fabricated with the n-i-p planar architecture FTO/TiO_2/perovskite/Spiro-OMeTAD (with and without AgI dopant)/MoO_3/Ag. As shown in Fig. 1, TiO_2 and Spiro-OMeTAD were used as the electron-transporting and the hole-transporting layer respectively. The chemical composition of the perovskite precursor is $CH_3NH_3PbI_3$ ($MAPbI_3$). In order to observe the influence of the doping of AgI on the morphology of the hole-transport layer, a comparison between the Spiro-OMeTAD without and with AgI dopant from the optical microscopy images was shown in Fig. 2. With the intervals for 48h, obvious changes occurred and more defects appeared on the surface of the doped Spiro-OMeTAD while pristine Spiro-OMeTAD kept a relatively better surface morphology with merely subtle changes. This clearly shows the doping of Ag^+ has a certain effect on the morphology, as well as performance of Spiro-OMeTAD film.

Atomic force microscopy (AFM) was utilized to study the influence of AgI doping on the Spiro-OMeTAD surface morphology. Pristine Spiro-OMeTAD showed a relatively homogeneous surface morphology with a root-mean-square (rms) roughness of 0.843 nm (Fig. 3). While the AgI doped Spiro-OMeTAD had a relatively higher roughness up to 1.80 nm. After 168 h aging for the undoped HTL the film had the roughness of 1.044 nm, which displayed subtle change of surface morphology. However, the AgI doped HTL shows more uneven hillocks in the film and inhomogeneous surface consistent with the increased roughness of 2.30 nm. This indicates that the introduction of Ag^+ into the hole-transport layer have a big impact on the morphology of Spiro-OMeTAD layer.

In order to investigate the effect of aging on the undoped and AgI doped perovskite films we performed UV-visible absorption spectroscopy and X-ray diffraction (XRD) measurements before and after 168 hours of aging. From the UV-visible absorption the structure with the Ag^+ doping didn't bring too obvious effects on the perovskite, comparing with that pristine structure (Fig. 4a), the incorporation of AgI affected the absorption of perovskite layer slightly. Similarly, no major difference was found in the X-ray diffraction spectra for the undoped and AgI doped perovskite films with the aging. Only reduced the intensity of peaks as an indication of degradation of perovskite films over time (Fig. 4b). This means that the degradation of AgI-doped perovskite didn't cause the formation of PbI_2, as in conventional process.

To check the influence of AgI doping on the device performance of PSCs, we studied the electrical properties of the device with and without AgI doping, with a structure of FTO/TiO_2/perovskite/Spiro-OMeTAD(with and without AgI dopant)/MoO_3/Ag. At the beginning, several controlled experiments conducted to explore the optimum doping concentration of AgI. Doping concentration of AgI varied from 1M%, 2M%, 3M% and 5M% respectively. The key parameters including open circuit voltage (V_{oc}) , short circuit current density (J_{sc}) , fill factor (FF) and PCE are summarized in Table 1, where the best doping ratio of AgI (3M%) in Spiro-MeOTAD was optimized based on the device performance. Besides, the photocurrent hysteresis phenomenon in devices was evaluated by recording the *J-V* curves with forward and reverse scan directions, as shown in Fig. S1 and table S1, which also explained that Spiro-OMeTAD:AgI(3M%) was considered as the best doping ratio in our work. A typical reference device based on the Spiro-OMeTAD HTL showed a V_{oc} of 1.06 V, a J_{sc} of 23.51

mA/cm^2 and FF of 68%, yielding a PCE of 16.95%. The champion device based on the AgI-doped (3M%) Spiro-OMeTAD HTL showed a V_{oc} of 1.03 V, a J_{sc} of 22.96 mA/cm^2, and an FF of 66% yielding a PCE of 15.58%. The current density-voltage (J-V) characteristic curves in the corresponding perovskite solar cells under AM 1.5 G irradiation of 100 mW/cm^2 are presented in Fig. 5a. Also, as shown by the PCE distribution histograms in Fig. 5b, over 20 perovskite solar cells were fabricated and tested to verify the high performance reproducibility of PSCs. The decreased device performance caused by Ag$^+$ doping also supports that the introduction of Ag$^+$ into the hole-transport layer has direct influence on the performance degradation in PSCs.

In addition, the aging experiments were conducted by keeping the doped and undoped devices in nitrogen atmosphere and in ambient air to study the long-term stability of PSCs. Fig. 5c and Fig. 5d display the evolution of PCE in air atmosphere and in nitrogen atmosphere, respectively. Noticeably, the device performance in ambient air was sensitive to degradation as compared to devices kept in nitrogen environment, Fig. 5c-d shows that the PCE of the device with Ag$^+$ doping in HTL decreased more dramatically than the device with no Ag$^+$ doping. It reveals that Ag electrode penetration into the adjacent hole transporting layer (HTL) in the PSCs does account for the device performance degradation.

To further reveal how Ag$^+$ ion penetration into the HTL deteriorates device performance, PSCs with a structure of ITO/PEDOT:PSS/Spiro-OMeTAD(with and without AgI dopant)/MoO_3/Ag were fabricated to quantitatively assess the density of defects. The typical double logarithmic current density-voltage *(J-V)* characteristics curves are plotted under the dark condition, shown in Fig. 5e and Fig. 5f, where typically three regions of *J-V* curves were observed in both devices. In low bias, there was a linear relationship between the current density and voltage. That is reflected an Ohmic contact with electrode. With increasing the bias, the sharp rise of J-V curves were associated with a trap-filled limit current, where all the defects are occupied by charge carriers. The defect density N could be calculated according to the equation $\mathrm{N} = 2\varepsilon\varepsilon_0 V_{TFL}/qd^2$, where and are the dielectric constants of Spiro-MeOTAD and the vacuum permittivity respectively, d is the thickness of HTL layer, q is the elementary charge and V_{TFL} is the intersection of two tangent lines from the J-V curve [26,27].The defect density in pristine Spiro-OMeTAD and AgI-doped Spiro-OMeTAD films was estimated to be 1.6×10^{15} cm^{-3} and 2.4×10^{15} cm^{-3} respectively. After the incorporation of Ag^+, the defect density was nearly increased by twice in the hole transporting layer. This further confirms that Ag penetration would lead to the deterioration of the device performance due to the increase of the defect density in the hole transporting layer.

4. Conclusions

In summary, we have demonstrated that Ag^+ penetration from Ag electrode into the adjacent hole-transporting layer in the PSCs is responsible for the degradation of solar cells and responsible for the detrimental factor for the long-term operational stability of PSCs. AgI doping has detrimental effect on the surface morphology of the Spiro-OMeTAD layer. In this study, the degradation of PSCs paves through the incorporation of Ag^+ into HTL causing more deep-level defects in the Spiro-OMeTAD layer and consequently caused a deterioration of the hole-transporting ability of Spiro-OMeTAD, leading to degradation of solar cell performance. The origin of this degradation root from the HTL/metal electrode interface is rather different from conventional degradation of PSCs which generally occurs due to degradation of perovskite active layer. The finding in this work proves a direct evidence of the degradation possibility caused by Ag electrode penetration.

Acknowledgements

We acknowledge financial support from the Natural Science Foundation of China (Nos. 61674109), the National Key R&D Program of China (No. 2016YFA0202400), and the Natural Science Foundation of Jiangsu Province (No. BK20130288), the Open Fund of the State Key Laboratory of Integrated Optoelectronics (IOSKL2018KF07)This project is also funded by the Collaborative Innovation Center of Suzhou Nano Science and Technology, and by the Priority Academic Program Development of Jiangsu Higher Education Institutions (PAPD).

Figures and Tables

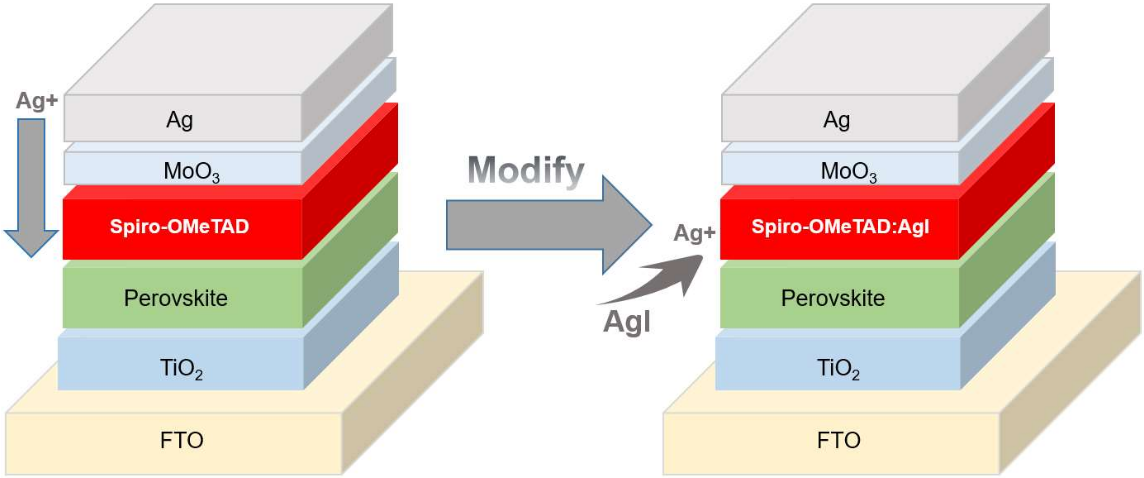

Fig. 1. Schematic diagram for the experiment: the effects of Ag^+ penetration from Ag electrode into the adjacent hole transporting layer (HTL) in the PSCs are magnified by directly doping Ag^+ into the Spiro-OMeTAD layer (HTL).

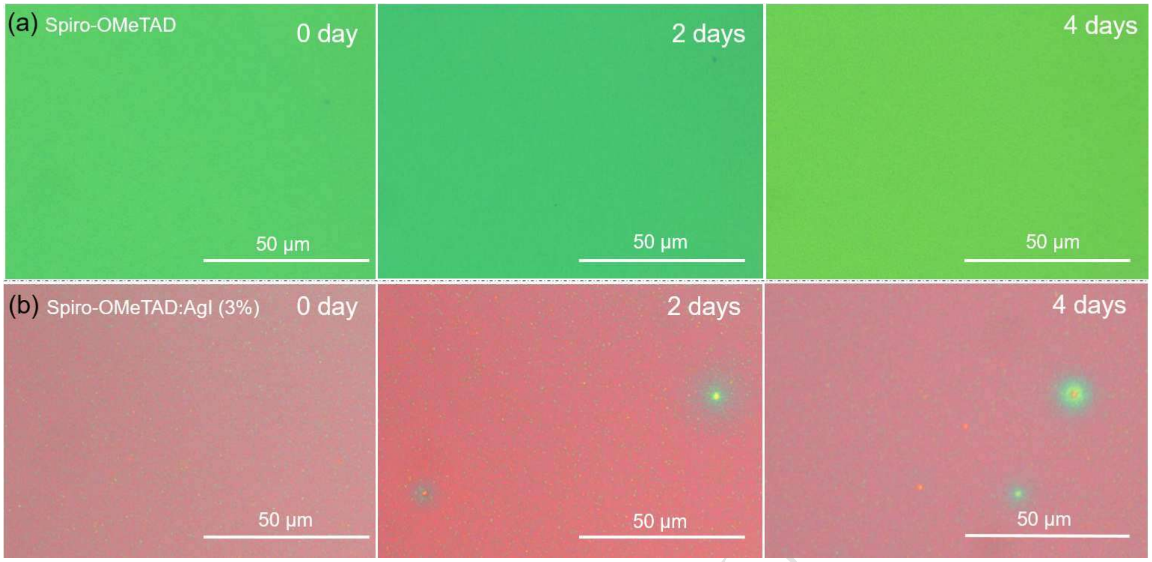

Fig. 2. Microcosmic images from optical microscope which display the change of films along time for (a) the pristine Spiro-OMeTAD and (b) Spiro-OMeTAD: AgI (3%).

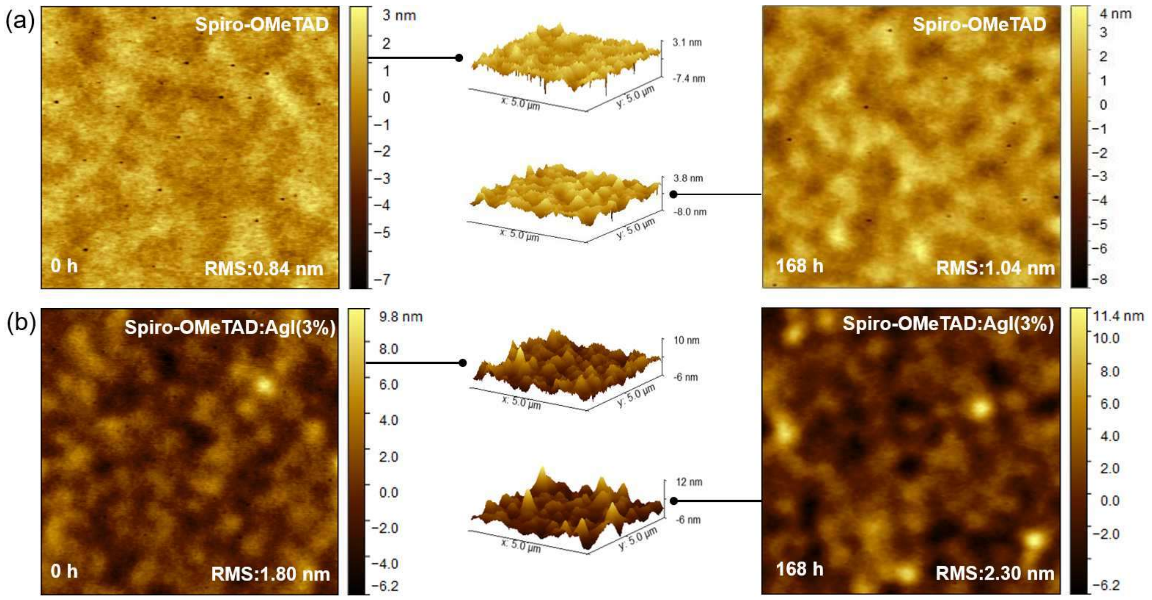

Fig. 3. AFM images of films which display the change of surface morphology along aged time (168 h) for (a) the pristine Spiro-OMeTAD and (b) Spiro-OMeTAD: AgI (3%).

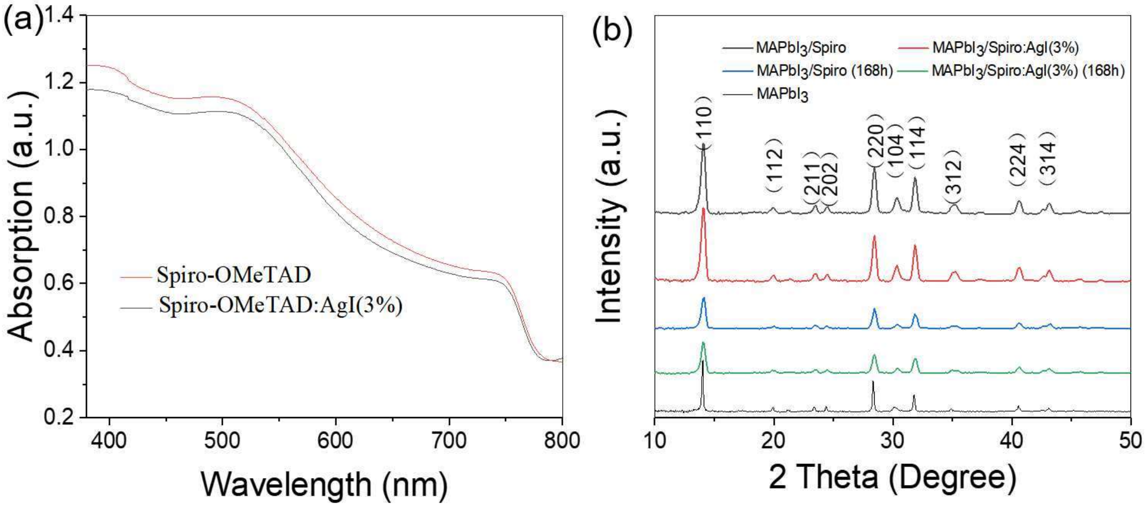

Fig. 4. (a) Absorption curves of perovskite films coated with HTLs of prisine Spiro-OMeTAD and Spiro-OMeTAD: AgI (3%); (b) the Comparison of X-ray diffraction images before and after 168h aging for Spiro-OMeTAD and Spiro-OMeTAD:AgI (3%).

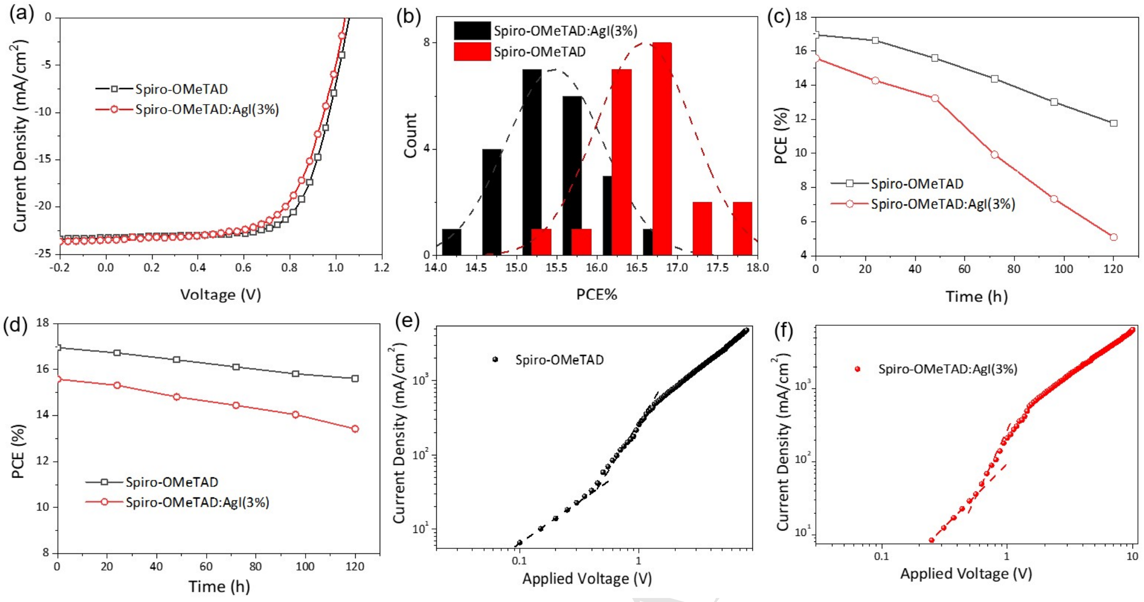

Fig. 5. (a) *J-V* characterizations curves of Spiro-OMeTAD and Spiro-OMeTAD:AgI (3%) based PSCs. (b) Histogram charts of the PCE statistics for Spiro-OMeTAD and Spiro-OMeTAD:AgI (3%) based PSCs; (c) PCE values aged in air as a function of time; (d) PCE values aged in nitrogen as a function of time; *J-V* curves in (e) Spiro-OMeTAD and (f) Spiro-OMeTAD:AgI (3%) based hole-dominated devices with a structure of ITO/PEDOT:PSS/HTL/MoO_3/Ag.

Table 1. Cell parameters of Spiro-OMeTAD: AgI based PSCs with varied doping concentration of AgI.

HTL	V_{oc} (V)	J_{sc} (mA/cm^2)	FF	PCE (%)
Spiro-OMeTAD	1.06	23.51	0.68	16.95
Spiro-OMeTAD: AgI (1 wt%)	1.02	22.50	0.63	14.46
Spiro-OMeTAD: AgI (2 wt%)	1.06	22.64	0.62	14.81
Spiro-OMeTAD: AgI (3 wt%)	1.03	22.96	0.66	15.58
Spiro-OMeTAD: AgI (5 wt%)	1.03	23.39	0.61	14.73

REFERENCES

[1] NREL Best Research Cell Efficiencies, http://www.nrel.gov/pv/assets/images/efficiency-chart.png (accessed: February 2019).

[2] A. Kojima, K. Teshima, Y. Shirai, T. Miyasaka, J. Am. Chem. Soc. 131 (2009) 6050-6051.

[3] D. W. Zhao, C. L. Wang, Z. N. Song, Y. Yu, C. Chen, X. Z. Zhao, K. Zhu, Y. F. Yan, ACS Energy Lett. 3 (2018) 305-306.

[4] R. K. Misra, S. Aharon, B. Li, D. Mogilyansky, I. Visoly-Fisher, L. Etgar, E. A. Katz, J. Phys. Chem. Lett. 6 (2015) 326-330.

[5] D. Koushik, W. J. Verhees, Y. Kuang, S. Veenstra, D. Zhang, M. A. Verheijen, M. Creatore, R. E. I. Schropp, Energy Environ. Sci. 10 (2017) 91-100.

[6] Y. Bai, Q. Dong, Y. Shao, Y. Deng, Q. Wang, L. Shen, D. Wang, W. Wei, J. Huang, Nat. Commun. 7 (2016) 12806.

[7] Y. Zhao, J. Wei, H. Li, Y. Yan, W. Zhou, D. Yu, Q. Zhao, Nat. Commun. **7** (2016) 10228.

[8] N. Aristidou, I. Sanchez-Molina, T. Chotchuangchutchaval, M. Brown, L. Martinez, T. Rath, S. A. Haque, Angew. Chem., Int. Ed. 127 (2015) 8326-8330.

[9] M. Li, Z. K. Wang, M. P. Zhuo, Y. Hu, K. H. Hu, Q. Q. Ye, S. M. Jain, Y. G. Yang, X. Y. Gao, L. S. Liao, Adv. Mater. 30 (2018) 1800258.

[10] Z. Y. Liu, K. K. Liu, H. H. Wang, S. M. Jain, J. J. Duan, T. W. He, R. M. Fan, J. E. Yang, H. R. Liu, F. P. Zhang, Sol. Energy 176 (2018) 1-9.

[11] S. H. Turren-Cruz, A. Hagfeldt, M. Saliba, Science 362 (2018) 449-453.

[12] Y. H. Lou, M. F. Xu, Z. K. Wang, S. Naka, H. Okada, L. S. Liao, Appl. Phys. Lett. 102 (2013) 113305.

[13] Y. H. Lou, M. Li, Z. K. Wang, Appl. Phys. Lett. 108 (2016) 053301.

[14] A. Guerrero, J. You, C. Aranda, Y. S. Kang, G. Garcia-Belmonte, H. Zhou, J. Bisquert, Y. Yang, ACS Nano 10 (2015) 218-224.

[15] J. M. Wang, Z. K. Wang, M. Li, C. C. Zhang, L. L. Jiang, K. H. Hu, Q. Q. Ye, L. S. Liao, Adv. Energy Mater. 8 (2018) 1701688.

[16] T. A. Berhe; W. N. Su, C. H. Chen, C. J. Pan, J. H. Cheng, H. M. Chen, M. C. Tsai, L. Y. Chen, A. A. Dubale, Energy Environ. Sci. 9 (2016) 323-356.

[17] Z. K. Wang, L. S. Liao, Adv. Optical Mater. 6 (2018) 1800276.

[18] H. D. Pham, T. T. Do, J. Kim, C. Charbonneau, S. Manzhos, K. Feron, W. C. Tsoi, J. R. Durrant, S. M. Jain, P. Sonar, Adv. Energy Mater. 8 (2018) 1703007.

[19] H. D. Pham, K. Hayasake, J. Kim, T. T. Do, H. Matsui, S. Manzhos, K. Feron, S. Tokito, T. Watson, W. C. Tsoi, J. Mater. Chem. C 6 (2018) 3699-3708.

[20] Y. C. Zhao, W. K. Zhou, H. R. Tan, R. Fu, Q. Li, F. Lin, D. P. Yu, G. Walters, H. S. Edward, Q. Zhao, J. Phys. Chem. C 121 (2017) 14517-14523.

[21] K. Domanski, J. P. Correa-Baena, N. Mine, M. K. Nazeeruddin, A. Abate, M. Saliba, W. Tress, A. Hagfeldt, M. Gratzel, ACS Nano 10(2016) 6306-6314.

[22] Q. Q. Ye, Z. K. Wang, M. Li, C. C. Zhang, K. H. Hu, L. S. Liao, ACS Energy Lett. 3 (2018) 875-882.

[23] T. Leijtens, G. E. Eperon, S. Pathak, A. Abate, M. M. Lee, H. J. Snaith, Nat. Commun. 4 (2013) 2885.

[24] Y. Han, S. Meyer, Y. Dkhissi, K. Weber, J. Pringle, U. Bach, L. Spiccia, Y. B. Cheng, J. Mater. Chem. A 3 (2015) 8139-8147.

[25] Y. Kato, L. K. Ono, M. V. Lee, S. Wang, S. R. Raga, Y. Qi, Adv. Mater. Interfaces 2 (2015) 1500195.

[26] Z. H. Liu, J. N. Hu, H. Y. Jiao, L. Li, G. H. J. Zheng, Y. H. Chen, Y. Huang, Q. Zhang, C. Shen, Q. Chen, H. P. Zhou, Adv. Mater. 29 (2017) 1606774.

[27] Y. H. Lou, M. F. Xu, L. Zhang, Z. K. Wang, S. Naka, H. Okada, L. S. Liao, Org. Electron. 14 (2013) 2698-2704.

Highlights

- AgI was doped into hole-transporting layer of Spiro-OMeTAD based on a solution-process.
- Ag^+ ion behavior in the perovskite solar cells was investigated.
- The incorporation of Ag^+ brought deep-level defects in the Spiro-OMeTAD layer and consequently caused a deterioration of the device.
- Understanding the impacts of the metal electrode penetration will promote advancing in the overall stability.